



# MULTIPLE RECOLLISION OF NONSEQUENTIAL DOUBLE IONIZATION PROCESS

Tran Ngoc Lien Huong, Truong Dang Hoai Thu, Pham Nguyen Thanh Vinh\*

Department of Physics, Ho Chi Minh University of Pedagogy, 280 An Duong Vuong St., District 5,  
Ho Chi Minh City, Vietnam

**Abstract:** We systematically investigate the contribution of recollision dynamics to the non-sequential double ionization process of the Ar atom for a wide range of laser intensity. The result shows that the first- and second-recollision scenarios have a significant contribution to the nonsequential double ionization vents (NSDI). Moreover, we figure out that the impact of double-recollision trajectories decreases as the laser intensity increases. Besides, many details of multiple recollisions are also investigated in this paper.

**Keywords:** non-sequential double ionization, multiple recollisions, classical ensemble model

## 1 Introduction

The interaction process between intense laser fields and atoms or molecules has led to many new physical phenomena, such as high harmonic generation (HHG) [9], above-threshold ionization (ATI) [6], and non-sequential double ionization (NSDI) [11, 20]. Among them, the NSDI process has been widely studied in several recent decades since it provides pure electron-electron ( $e-e$ ) correlated dynamics in the atomic or molecular orbitals toward the recollision process. At present, the widely accepted picture for NSDI has been well understood by using the quasi-classical rescattering model [3]: the first ionized electron, after being accelerated in the laser field for a fraction of an optical cycle, can be driven back by the oscillating laser field and recollide with its parent ion core. The NSDI was first discovered by Suran and Zapesochny for alkaline earth atoms in early 1975 [15]. Then this phenomenon quickly attracts the attention of the scientists since there exist experimental results that challenge the contemporary knowledge. For instance, at high laser intensity, the V-like structure [14] in the correlated electron momentum spectra was experimentally observed. In case of low laser intensity, theoretical studies have demonstrated that both nuclear Coulomb attraction and the final-state electron repulsion contribute to this structure [19]. However, for high laser intensity, the root of V-like is the asymmetric energy sharing process between recolliding and bounded electrons during the recollision process [20]. Recently, the cross-shape structure in two electron momentum spectra of Ar has been experimentally observed [2]. This is a special structure and has not been previously observed. Remarkably, in this study, the authors use near-single-cycle laser pulses to eliminate the impact of secondary recollisions.

---

\* Corresponding: [vinhpham@hcmup.edu.vn](mailto:vinhpham@hcmup.edu.vn)

In the recollision model, the ionized electron driven by the linearly polarized laser pulse can return many times to the parent ion in case of many-cycle laser pulses, and such situation is called multiple recollisions. In the NSDI, multiple recollisions are only speculated. However, experimental results show that multiple recollisions strongly contribute to NSDI spectrum; for example, the observed anticorrelated behavior in the correlated electron momentum spectrum and the high energy cutoff in the sum-energy spectrum of NSDI at the low laser intensity regime [18] are similar to the multiple-recollision induced low-energy structures in strong-field above-threshold ionization [10]. Besides, currently, there are few theoretical calculations to explore multiple recollisions [11].

In this paper, with the three-dimension classical ensemble model, we provide a systematic investigation of the recollision dynamics in the NSDI of Ar induced by many-cycle laser pulses for a wide range of laser intensities which are able to produce the recolliding electrons whose energies are well below, at, and above the recollision-ionization threshold of Ar. By tracing of the NSDI trajectories, we deeply study the dependence of multiple recollisions on laser intensity, as well as the dynamics of multiple recollisions process.

## 2 Three-dimension classical ensemble model

Numerically, there are two methods to approach the NSDI process: the first method is based on the solutions of the time dependent Schrödinger equation (TDSE) governing the interaction between atoms or molecules with the laser field. This is obvious that the method provides the exact and most reliable data. However, such consideration is extremely tedious by mean of programming [13] and computer-resource demand. The second approach is the classical ensemble model. Since being introduced in 2001 [12], the three-dimensional ensemble model has been considered as a powerful approach in studying strong-field double ionization (DI) [7, 19]. In that model, the evolution of the two-electron system is governed by Newton classical equations of motion (atomic units are used throughout this paper unless stated otherwise)

$$\frac{d^2 \vec{r}_i}{dt^2} = -\vec{\nabla} [V_{ne}(r_i) + V_{ee}(r_1, r_2)] - \vec{E}(t), \quad (1)$$

where subscript  $i$  is the label representing two electrons,  $\vec{r}_i$  is the coordinate of the  $i$ th electron, and  $\vec{E}(t)$  is the electric field which is chosen to be linearly polarized along the  $x$  axis and has the wavelength 780 nm of trapezoidal shape with ten optical cycles including two cycles turning on, six cycles at full strength, and two cycles turning off. In this paper, the peak intensities of the laser pulse are chosen to be  $0.8 \times 10^{14}$  W/cm<sup>2</sup>,  $1.5 \times 10^{14}$  W/cm<sup>2</sup> and  $2.5 \times 10^{14}$  W/cm<sup>2</sup> that enable to produce the recolliding electrons whose energies are well below, at, and above the recollision-ionization threshold of argon, respectively. Here  $V_{ne}(\mathbf{r}_i) = -2 / \sqrt{\mathbf{r}_i^2 + a}$  and  $V_{ee}(\mathbf{r}_1, \mathbf{r}_2) = 1 / \sqrt{(\mathbf{r}_1 - \mathbf{r}_2)^2 + b}$  are the ion-electron attractive potential and the electron-electron ( $e$ -

e) repulsive potential, respectively. Note that for avoiding autoionization, soft parameters  $a = 1.5^2$  and  $b = 0.1^2$  are used without any loss of physical properties [11].

To solve equation (1), we need to obtain the initial conditions. In the classical model, atoms and molecules are characterized solely by the ionization energy which is equal to  $-1.59$  a. u. in case of Ar, corresponding to the summation of the first and second ionization potentials. The available kinetic energy is distributed randomly between two electrons in the momentum space. Then, the system is allowed to evolve in a sufficiently long time (200 a. u.) in the absence of the laser field to obtain stable position and momentum distributions [16, 20]. After obtaining initial conditions, we proceed to numerically solve equation (1) for an individual atom in the influence of the laser field using the fourth order Runge-Kutta method. At the end of the pulse, the energies of two ionized electrons are analyzed as

$$E_1 = \frac{v_{x1}^2}{2} + \frac{v_{y1}^2}{2} + \frac{v_{z1}^2}{2} - \frac{2}{\sqrt{x_1^2 + y_1^2 + z_1^2 + a}} + \frac{1}{2\sqrt{(x_1 - x_2)^2 + (y_1 - y_2)^2 + (z_1 - z_2)^2 + b}}, \quad (2a)$$

$$E_2 = \frac{v_{x2}^2}{2} + \frac{v_{y2}^2}{2} + \frac{v_{z2}^2}{2} - \frac{2}{\sqrt{x_2^2 + y_2^2 + z_2^2 + a}} + \frac{1}{2\sqrt{(x_1 - x_2)^2 + (y_1 - y_2)^2 + (z_1 - z_2)^2 + b}}, \quad (2b)$$

where  $x_i, y_i, z_i$  and  $v_{xi}, v_{yi}, v_{zi}$  are the drift positions and velocities of electron  $i^{\text{th}}$  in Cartesian coordinates, respectively. The atom is considered to be doubly ionized only if the energies of both electrons are positive [16, 20]. Note that in the framework of the classical model, both ionized electrons are set free via over-the-barrier mechanism.

### 3 Numerical results and discussion

We proceed to discuss the NSDI process of Ar induced by laser pulses having the parameters in section 2. Here we refer the first and second ionized electrons as recolliding and bounded electrons, respectively. Figure 1 shows the correlated two-electron momentum distribution (CTEMD) along the polarization axis of the laser field for different intensities:  $I = 0.8 \times 10^{14}$  W/cm<sup>2</sup> (Figure 1a–1c),  $I = 1.5 \times 10^{14}$  W/cm<sup>2</sup> (Figure 1d–1f) and  $I = 2.5 \times 10^{14}$  W/cm<sup>2</sup> (Figure 1g–1i). The left, middle, and right columns portray the total events, events relating to the trajectories which have only one recollision, and events associating with the ones which have two recollisions, respectively. In the following, we refer trajectories having one and two recollision events to single- and double-recollision trajectories, respectively. For the lowest laser intensity  $I = 0.8 \times 10^{14}$  W/cm<sup>2</sup>, the CTEMMD exhibits a prominently anti-correlated behavior, i.e. two electrons are liberated from the parent ion with similarly-drift momenta but in opposite directions, as shown in Figure 1a. For the moderate intensity of  $I = 1.5 \times 10^{14}$  W/cm<sup>2</sup>, the CTEMMD displays a clear double-line structure which is parallel to the main diagonal and observed experimentally by Eremina (see Fig. 1d) [4]. While for the highest laser intensity of  $I = 2.5 \times 10^{14}$  W/cm<sup>2</sup> (see Fig. 1g), the CTEMMD performs a V-like structure which is almost equivalent to the cross-shaped structure observed experimentally by Bergues [2]. Note that the CTEMMD in this

sufficiently high-intensity case is not symmetric with respect to the secondary diagonal line due to the early phase ionization of the atom. The explanation of those behaviors is postponed to our next project, and in this paper we concentrate on the contribution of the single- and double-recollision to the NSDI. By tracing these NSDI trajectories, we figure out that there are many multiple recollision trajectories, i.e. the recolliding electron recollides with the parent ion many times and transfers significant energy for the bounded one toward the recollision process. Note that the recollision time is defined as the instant when the recolliding electron enters the core area so that the distance between two electrons is less than 2.0 a. u. [11]. Our calculations show that only single- and double-recollision mainly contribute to the NSDI events. Obviously, from Figure 1, the contribution of single-recollision is universally predominant for all laser intensities. However, careful inspection discovers that the contribution of double-recollision decreases as the laser intensity increases. This contention can be observed from Figure 1c, 1f, and 1i in which the CTEM associated with double-recollision is more faded with respect to the increase of the field intensity.

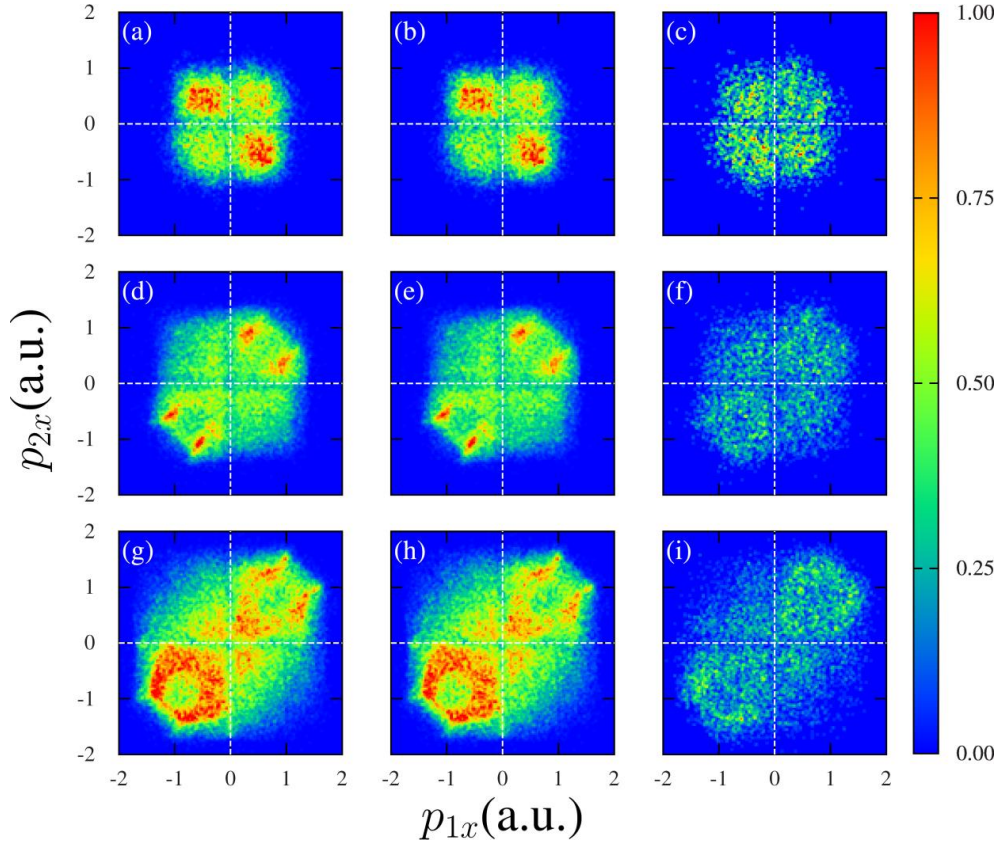


**Fig. 1.** Correlated two electron momentum distribution along the laser's polarization axis of laser field for three representative intensities:  $I = 0.8 \times 10^{14}$  W/cm<sup>2</sup> (a-c),  $I = 1.5 \times 10^{14}$  W/cm<sup>2</sup> (d-f) and  $I = 2.5 \times 10^{14}$  W/cm<sup>2</sup> (g-i). The left, middle and right columns show the correlated two-electron momentum distribution for all trajectories, single-recollision trajectories, and double-recollision trajectories, respectively.

In order to further explore the NSDI events, we proceed to analyze the evolution of the energies of two electrons during the interaction with laser field for three representative intensities as in Figure 1 and shown in Figure 2 for both cases of single- and double-recollision sample trajectories at the first and later return. Figure 2 provides an intuitive picture for all circumstances of the recollision process. In case of single-recollision, the only recollision occurs at the first return (first column) or third return for low intensity, second or third return for sufficiently high intensity (second column). We also notice that the instant of the first ionization event arises earlier for higher laser intensity, so does the returning instant (see the left shift of both instants marked in Figure 2 from the top to the bottom of the first and second column). This is straightforward to understand since the atom is more sensitive to be ionized as the laser intensity grows. A similar trend holds for double-ionization situations (see the third and fourth column in Figure 2). Another interesting feature that can be deduced from Figure 2 is the transition of NSDI mechanisms as the laser intensity varies. For low intensity below the recollision-ionization threshold, the dominant mechanism of NSDI is the recollision-induced excitation with subsequent ionization (RESI) including the existence of a doubly excited state [5, 8]. Here the recolliding electron (solid red curve) enables to excite the bounded one (dashed blue curve) and is also trapped by the parent ion to temporarily settle in an excited state together with this bounded electron (see the top row). For moderate intensity at the threshold (middle row), the dominant mechanism of NSDI is still RESI, however, in this case, there is no continuation of the doubly excited state since the recolliding electron has enough energy to kick out the bounded one with the expense of being captured by the parent ion for a while. When further increasing the laser intensity (bottom row), the dominant mechanism of NSDI is  $(e, 2e)$  in which the recolliding electron directly promotes the bounded one into the continuum via electron impact ionization [2].

For double-recollision trajectories, we consider energies of two electrons in two cases: the first recollision occurs at the first returning and the second recollision occurs at the second or third returning for intensities  $I = 0.8 \times 10^{14} \text{ W/cm}^2$  (Figure 2c, 2d),  $I = 1.5 \times 10^{14} \text{ W/cm}^2$  (Figure 2g, 2h), and  $I = 2.5 \times 10^{14} \text{ W/cm}^2$  (Figure 2k, 2l). The results show at the first recollision that the energy exchange between recolliding and bounded electrons decreases when increasing the laser intensity. In order to further understand the double-recollision, we proceed to analyze the returning energies of recolliding electrons at the first and second return for three representative intensities as in Figure 1 and shown in Figure 3. Figure 3 indicates that the energy of the second return is less than that of the first return which is in good consistency with the scenario proposed by Simpleman's theory [17]. Moreover, when increasing laser intensity, the returning energy at the first recollision increases. Therefore, the recolliding electron moves so fast through the vicinity of the ion core and effectively transfers a small portion of its energy to the bounded electron. This explains that for high laser intensity, the impact of second returning trajectories becomes more significant.

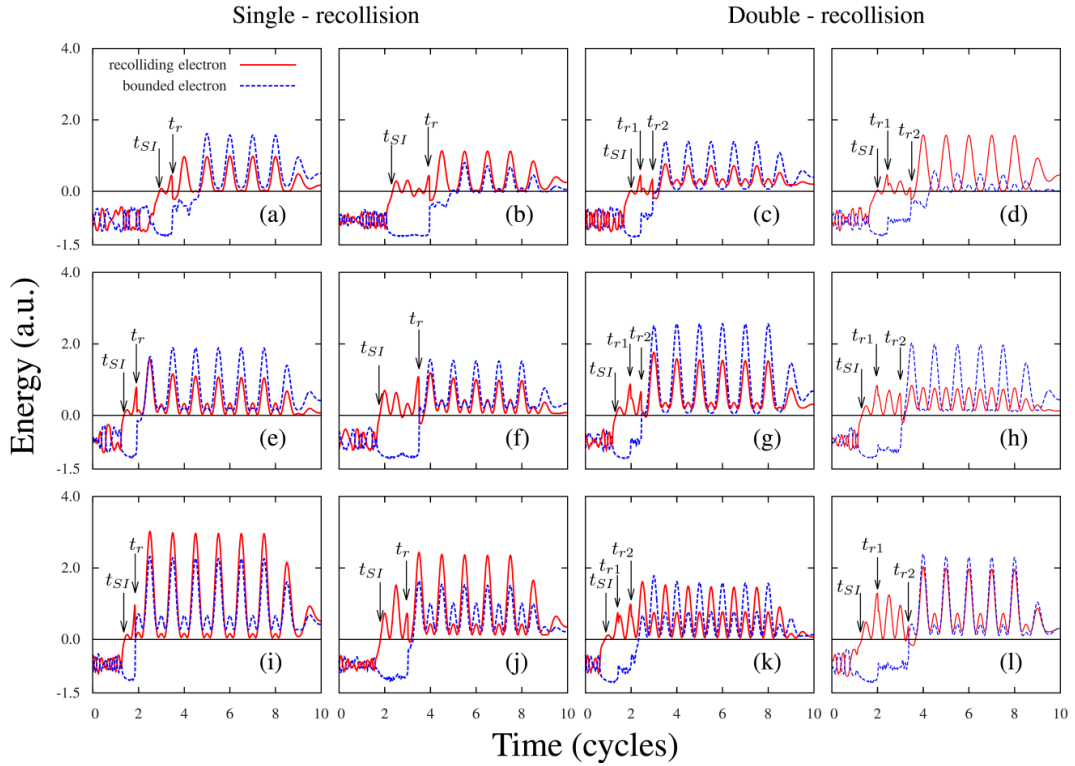


**Fig. 2.** Energies of two electrons during interaction process with laser field for intensities  $I = 0.8 \times 10^{14}$  W/cm<sup>2</sup> (a–d),  $I = 1.5 \times 10^{14}$  W/cm<sup>2</sup> (e–h) and  $I = 2.5 \times 10^{14}$  W/cm<sup>2</sup> (i–l). The first and second columns show energies of two electrons in single-recollision corresponding to the recollision occurring at the first and third return, respectively. The third and fourth column show energies of two electrons in double-recollision corresponding to the recollision occurring at the first and third return, respectively.

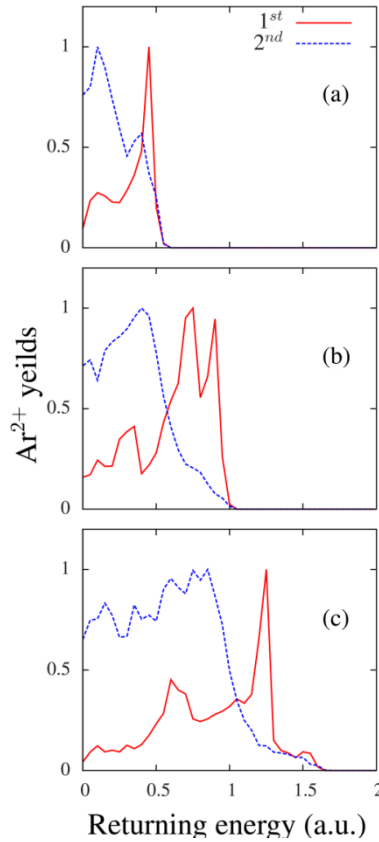


**Fig. 3.** Returning energies of recolliding electrons for double-recollision trajectories at first and second recollision for intensities  $I = 0.8 \times 10^{14} \text{ W/cm}^2$  (a),  $I = 1.5 \times 10^{14} \text{ W/cm}^2$  (b) and  $I = 2.5 \times 10^{14} \text{ W/cm}^2$  (c)

Figure 4 presents the traveling time for single- and double-recollision trajectories for three laser intensities  $I = 0.8 \times 10^{14} \text{ W/cm}^2$ ,  $I = 1.5 \times 10^{14} \text{ W/cm}^2$  and  $I = 2.5 \times 10^{14} \text{ W/cm}^2$ . Note that the traveling time is defined as a time difference between the first ionization moment and the recollision instant leading to NSDI. The result shows, for the single-recollision case at a low intensity, that the traveling time which focuses around  $0.4T_0$ ,  $1.65T_0$  and  $2.65T_0$  with  $T_0$  is the laser period, which correspond to the recollisions occurring at the first, third, and fifth returns, respectively (Figure 4a). The impact from the second and fourth return is negligible. The result also indicates that recolliding electrons mostly return at the first return. According to recollision picture, recolliding electrons return with the highest possibility at the first return and second highest possibility at the third return [1]. Therefore, our result is again well consistent with this model. When the intensity increases, the second and fourth returns appear, since recolliding electrons return with sufficiently large energy to liberate the bounded electron. In case of double-recollision trajectories, at low intensity (Figure 4b), the traveling time distribution for the first recollision mainly locates around  $0.55T_0$ , corresponding to the recollision at the first return, while, for the second recollision, the distribution is shifted by  $0.4T_0$  and has a relatively

uniform distribution for the later returns. These results show that the second recollision mainly occurs at the next return after the first one.

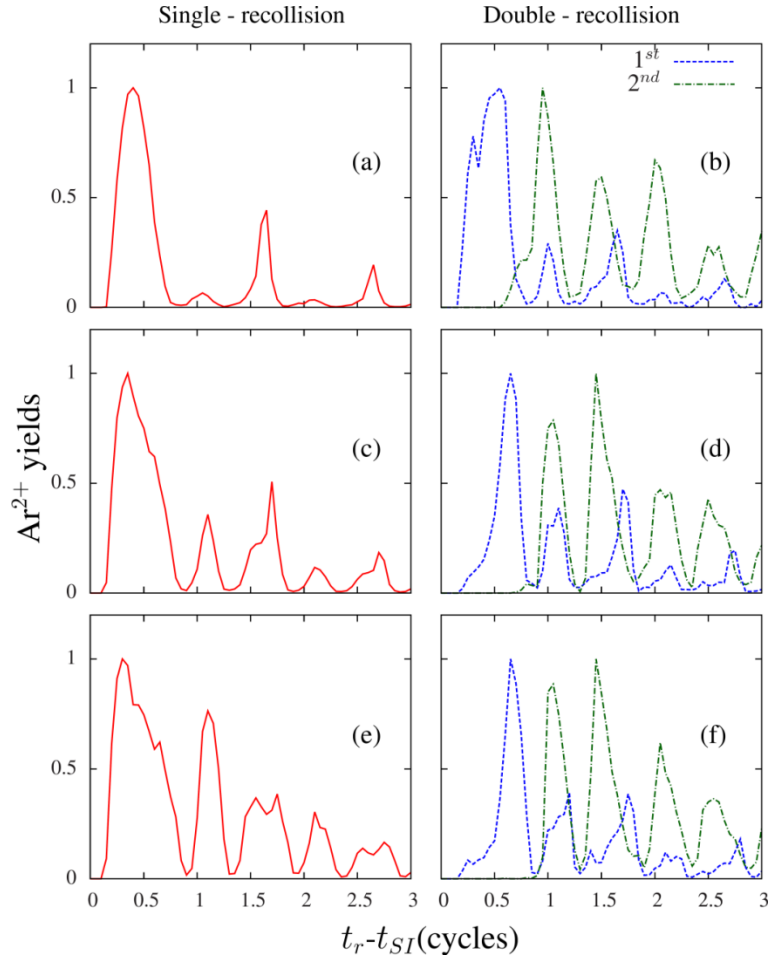


**Fig. 4.** Traveling time distribution for three representative intensities  $I = 0.8 \times 10^{14} \text{ W/cm}^2$  (a–b),  $I = 1.5 \times 10^{14} \text{ W/cm}^2$  (c–d) and  $I = 2.5 \times 10^{14} \text{ W/cm}^2$  (e–f). The first and second columns correspond to the situation for single and double recollision trajectories, respectively.

Finally, the time difference between two recollision moments for double-recollision trajectories as well as the time delay between the last recollision and DI moment for both single- (solid red curve) and double-recollision (dashed blue curve) trajectories for three representative laser intensities as in Figure 1 is shown in Figure 5. The time difference in case of lowest laser intensities peaks around  $0.4T_0$ ,  $1.0T_0$  and  $1.65T_0$ . Then, only the first and second peaks of time difference maintain when increasing laser intensity and the highest peak is always the first one confirming that the second recollision mainly occurs at the next return after the first one. In case

of a time delay between the recollision and the DI moment, for the lowest laser intensity, this time delay of double-recollision trajectories is smaller than that of single-recollision trajectories at the first peak (see Figure 1b). Besides, at next peaks, the  $\text{Ar}^{2+}$  yields of double-recollision events become lower. These results show that the NSDI process occurs more quickly for double-recollision trajectories. When laser intensity is higher, the time delay of single-recollision trajectories is similar to that of double-recollision trajectories. Moreover, this time delay focuses mainly from 0 to  $0.4T_0$  once again confirming that  $(e, 2e)$  mechanism is more dominant than RESI mechanism for high laser intensity.

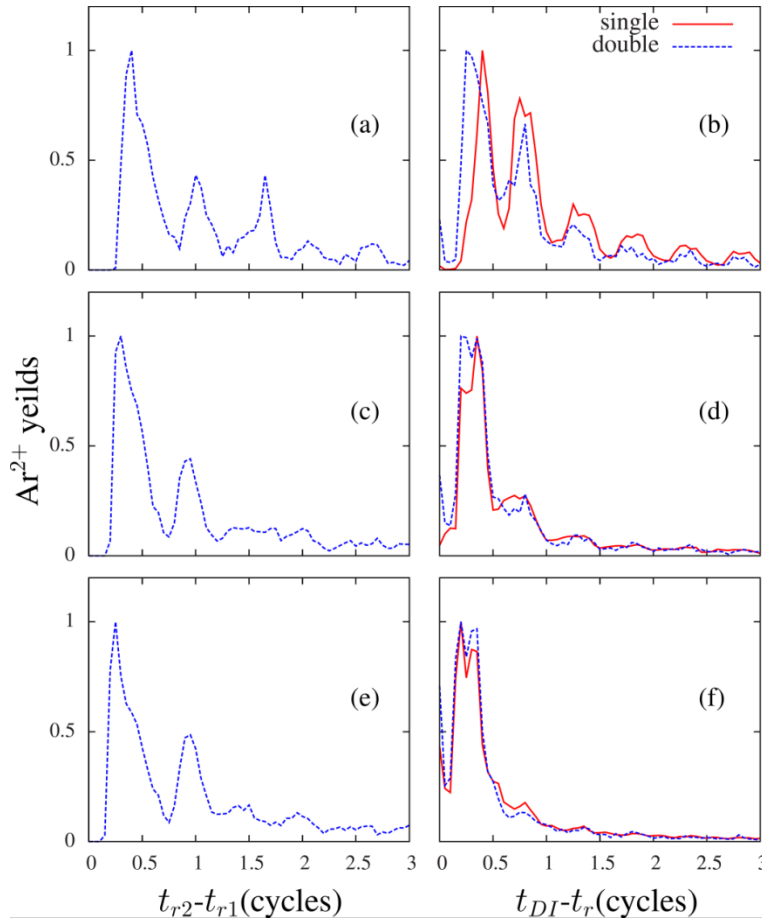


**Fig. 5.** Time difference between two recollision moments for double recollision trajectories (first column) as well as time delay between last recollision and DI moment (second column) for both single- (solid red curve) and double-recollision (dashed blue curve) trajectories for three laser intensities:  $I = 0.8 \times 10^{14}$  W/cm<sup>2</sup> (a-b),  $I = 1.5 \times 10^{14}$  W/cm<sup>2</sup> (c-d) and  $I = 2.5 \times 10^{14}$  W/cm<sup>2</sup> (e-f)

## 4 Conclusion

In this paper, by using a three-dimensional classical ensemble model, we investigate the dependence of multiple recollision dynamics in the strong-field NSDI on laser intensity. At low intensity, the returning energy of the first ionized electron is very low, thus the contribution from secondary recollisions is indispensable. When increasing laser intensity, the contribution from multiple recollisions decreases since the energy of returning electron is sufficiently large to lead the NSDI at the first recollision. Moreover, we intuitively demonstrate, by tracing the evolution of the energies of two electrons during the interaction with the laser pulse, that at low intensity, the NSDI process occurs solely by recollision-induced excitation, followed by subsequent ionization including the existence of a doubly-excited state. However, in case of higher laser intensity, ( $e$ ,  $2e$ ) mechanism becomes dominant. Several details of multiple recollision are also clearly analyzed in this paper.

## References

1. Becker W., Grasbon F., Kopold R., Milosevic D., Paulus G., and Walther H. (2002), "Above-threshold ionization: From classical features to quantum effects", *Adv. At. Mol. Opt. Phys.* **48**, 35.
2. Bergues B., Kübel M., Johnson Nora G., Fischer B., Camus N., Betsch Kelsie J., Herrwerth O., Senftleben A., Saylor A. M., Rathje T., Pfeifer T., Ben-Itzhak I., Jones Robert R., Paulus Gerhard G., Krausz F., Moshhammer R., Ullrich J. and Kling Matthias F. (2012), "Attosecond tracing of correlated electron-emission in non-sequential double ionization", *Nature Communications* **3**, 813.
3. Corkum P. B. (1993), "Plasma perspective on strong field multiphoton ionization", *Physical Review Letters* **71**, 1994–1997.
4. Eremina E., Liu X., Rottke H., Sandner W., Dreischuh A., Lindnery F., Grasbony F., Paulusy G. G., Walthery H., Moshhammer R., Feuersteinz B. and Ullrich J. (2003), "Laser induced nonsequential double ionization investigated at and below the threshold for electron impact ionization", *Journal of Physics B* **36**.
5. Feuerstein B., Moshhammer R., Fischer D., Dorn A., Schröter C. D., Deipenwisch J., Crespo Lopez-Urrutia J. R., Höhr C., Neumayer P., Ullrich J., H. Rottke, Trump C., Wittmann M., Korn G., and Sandner W. (2001), "Separation of recollision mechanisms in nonsequential strong field double ionization of Ar: The role of excitation tunneling", *Physical Review Letter* **87**, 043003–4
6. Gontier Y., Poirier M., and Trahin M. (1980), "Multiphoton absorptions above the ionisation threshold", *Journal of Physics B* **13**, 1381.
7. Hann S. L., Dyke J. S. Van, and Smith Z. S. (2008), "Recollision excitation, electron correlation, and the production of high-momentum electrons in double ionization", *Physical Review Letter* **101**, 113001.
8. Kopold R., Becker W., Rottke H. and Sandner W. (2000), "Routes to nonsequential double ionization", *Physical Review Letter* **85**, 3781–3784.
9. Le V. H, Le A. T., Rui-Hua Xie, and Lin C.D. (2007), "Theoretical analysis of dynamic chemical imaging with lasers using high-order harmonic generation", *Physical Review A* **76**, 013414–13.

10. Liu Y., Tschuch S., Rudenko A., Dürr M., Siegel M., Morgner U., Moshhammer R., and Ullrich J. (2008), "Strong-Field Double Ionization of Ar below the Recollision Threshold", *Physical Review Letter* **101**, 053001–4.
11. Ma X., Zhou Y. and Lu P. (2016), "Multiple recollisions in strong-field nonsequential double ionization", *Physical Review A* **93**, 013425–6.
12. Panfili R., J. Eberly H., and Haan S. L. (2001), "Comparing classical and quantum dynamics of strong-field double ionization", *Optics Express* **8**, 431.
13. Parker J. S., Doherty B. J. S., Taylor K. T., Schultz K. D., Blaga C. I, and DiMauro L. F. (2006), "High-Energy Cutoff in the Spectrum of Strong-Field Nonsequential Double Ionization" , *Physical Review Letter* **96**, 133001–4.
14. Rudenko A., De Jesus V. L. B., Ergler Th., Zrost K., Feuerstein B., Schröter C. D., Moshhammer R., and Ullrich J. (2007), "Correlated two-electron momentum spectra for strong-field nonsequential double ionization of He at 800 nm", *Physical Review Letter* **99**, 263003–4.
15. Suran V. V., and Zapesochny I. P. (1975), "Observation of  $\text{Sr}^{2+}$  in multiple-photon ionization of strontium", *Sov. Tech. Phys. Letters* **1**, 420.
16. Truong Thu D. H., Huynh Son V., and Pham Vinh N. T. (2015), "V-like structure in the correlated electron momentum distribution for nonsequential double ionization of helium", *Journal of Science of Ho Chi Minh University of Education* **5**, 26.
17. van Linden van den Heuvell, H. B. & Muller, H. G. *Of referencing in Multiphoton Processes* (ed. Smith, S. J. & Knight, P. L.) 25–34 (Cambridge University Press, 1988).
18. Wu C. Y., Yang Y. D., Liu Y. Q., Gong Q. H., Wu M. Y., Liu X., Hao X. L., Li W. D., He X. T., and Chen J. (2012), "Characteristic Spectrum of Very Low-Energy Photoelectron from Above-Threshold Ionization in the Tunneling Regime", *Physical Review Letter* **109**, 043001–5.
19. Ye D. F., Liu X., and Liu J. (2008), "Classical trajectory diagnosis of a fingerlike pattern in the correlated electron momentum distribution in strong field double ionization of Helium", *Physical Review Letter* **101**, 233003.
20. Zhou Y., Qing L. and Lu P. (2010), "Asymmetric electron energy sharing in strong-field double ionization of helium", *Physical Review A* **82**, 053402–5.